

Influence of Dispersion on Photon Number Distribution over the Parametric Modes of a Synchronously Pumped Optical Parametric Oscillator

© D.M. Malyshev, V.A. Averchenko, K.S. Tikhonov

St. Petersburg State University,
St. Petersburg, Russia
e-mail: malyshev.wrk@yandex.ru

Received July 20, 2025

Revised July 30, 2025

Accepted August 12, 2025

We describe influence of the group velocity dispersion on the photon number in the eigenmodes of a synchronously pumped optical parametric oscillator. Using the existing model taking into account the influence of quadratic dispersion on the evolution of the parametric modes, we analyze the processes involved in the redistribution of the mean photon number over the output radiation modes. Based on the fourth order perturbative solution for the field amplitude at the resonator output we numerically investigate the processes occurring in the optical oscillator.

Keywords: squeezed light, parametric down-conversion, group-velocity dispersion, optical parametric oscillator, nonclassical states of light, multimode light radiation.

DOI: 10.61011/EOS.2025.08.62023.8415-25

Introduction

Multimode squeezed light [1] is a key resource in the creation of quantum communication networks [2,3], in continuous-variable quantum computing [4,5], as well as in quantum cryptography [6]. The use of such light allows for increasing the precision of quantum metrology methods [7,8], spectroscopy [9], and time measurement [10]. Furthermore, squeezed light is employed to enhance the sensitivity of gravitational wave detectors [11] due to its capability to reduce vacuum noise, which hinders the measurement of small deviations in the arms of an interferometer-detector.

The most commonly used method for producing squeezed states of light is spontaneous parametric down-conversion (SPDC), in which a high-energy pump photon decays in a nonlinear crystal into two photons, signal and idler modes, under the fulfillment of phase-matching and wave synchronization conditions. This process enables the generation of nonclassical radiation in both pulsed and continuous-wave regimes. Squeezed light is obtained using various optical configurations such as optical parametric generators and various integrated circuits [12]. The use of different setups allows control over both the spatiotemporal characteristics and the modal structure of the generated radiation [13–17]. This provides the necessary flexibility in producing different quantum properties of light that meet the requirements of an experiment or specific applied tasks.

Experimentally and theoretically, it has been shown that an optical parametric generator with synchronous pumping (SPOPO), the scheme of which is shown in Fig. 1, generates multimode quadrature-squeezed radiation [18,19]. In the

time domain, the radiation obtained by SPOPO presents a sequence of equidistant femtosecond pulses. Each such pulse is a linear combination of independent broadband quadrature-squeezed modes. In the frequency domain, the spectrum of the generated light can be represented as a set of frequency combs, each corresponding to a distinct quantum parametric oscillator. The resulting radiation possesses a number of unique properties that make it valuable for solving various quantum-optical tasks.

One of these tasks is the synchronization of remote atomic clocks, which uses short optical pulses with reduced noise in quadratures [20,21]. Another application of squeezed light is the measurement of spectral properties of frequency combs, where it enables surpassing the standard quantum limit in measuring average energy, central frequency, and spectral bandwidth of ultrafast pulses [22]. Moreover, the presence of quantum correlations between

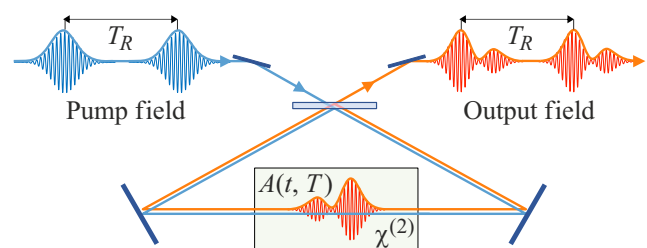


Figure 1. Schematic diagram of a synchronously pumped optical parametric generator (SPOPO). The pump field (blue) enters the resonator through a partially transparent mirror, then reaches the nonlinear $\chi^{(2)}$ -crystal, where the generation of the signal field (red) takes place.

frequency modes allows obtaining multipartite quantum-entangled cluster states based on them, which serve as a resource for one-way quantum computing [23,24] and measurement-based quantum networks [25–27].

The process of generating quadrature-squeezed light in a nonlinear crystal is subject to the influence of many factors, including the parameters and structure of the used resonator, the geometry of the crystal itself, and the properties of the intracavity medium. A detailed understanding of the light generation process in SPOPO is important to ensure effective control over the characteristics of its radiation, increased degree of squeezing, and subsequent transformations of the radiation in various applications.

In this study, the generation of multimode squeezed light under the presence of uncompensated group velocity dispersion in the SPOPO cavity is considered. The main task is to study the influence of quadratic dispersion on the average photon number in parametric light modes. The article is organized as follows. First, we briefly discuss the model of signal radiation generation in SPOPO introduced in [28]. Then the parameters defining the system's properties in its numerical modeling are established. Finally, we calculate how group velocity dispersion affects the photon distribution across the radiation modes.

Parametric modes in SPOPO

The generation of light in SPOPO in the time domain is described as follows.

The pump pulse passes into the resonator cavity through a partially transparent mirror, whose reflection and transmission coefficients are \mathcal{R} and \mathcal{T} respectively, and reaches the nonlinear crystal where the process of spontaneous parametric scattering of pump photons into pairs of lower-energy signal photons occurs. In this paper, we consider the case of degenerate parametric generation in a single spatial and single polarization mode of the field. It is assumed that the pump radiation is not supported by the resonator. When the signal pulse reaches the input mirror, part of the pulse leaves the resonator while the remainder continues circulating and again reaches the crystal synchronously with the arrival of the next pump pulse, which makes the generation process more efficient.

As the signal pulses propagate in the resonator medium, they undergo group velocity dispersion, which results in their dispersive broadening. The described quantum system can be modeled using the Heisenberg-Langevin equation, which describes the evolution of the quantum-mechanical operator of the slowly varying amplitude of the signal pulse $\hat{A}(t, T)$, circulating inside the resonant cavity. In the limit of weak nonlinear conversion and small group velocity

dispersion, the governing equation takes the form [28]:

$$\frac{\partial \hat{A}(t, T)}{\partial T} = \left(-\frac{\gamma}{2} + i\Delta - iD \frac{\partial^2}{\partial t^2} \right) \hat{A}(t, T) + \frac{1}{2} \int G(t, t') \hat{A}^\dagger(t', T) dt' + \sqrt{\frac{\gamma}{T_R}} \hat{A}^{\text{in}}(t, T). \quad (1)$$

The operator $\hat{A}(t, T)$ of the slow amplitude of the signal field obeys the standard bosonic commutation relations:

$$[\hat{A}(t, T), \hat{A}^\dagger(t', T')] = T_R \delta(t - t') \delta(T - T').$$

The slow time variable T describes the pulse evolution on times much longer than the cavity round-trip time T_R and the operator $\hat{A}(t, T = NT_R)$ defines the amplitude of the pulse after N round-trips of the resonant cavity. Due to the leakage of part of the pulse through the partially transparent mirror, the signal field in the resonant cavity undergoes decay at a rate $\gamma/2 = (1 - \sqrt{\mathcal{R}})/T_R$. The used model also takes into account the detuning $\Delta = \sqrt{\mathcal{R}}k(\omega_0)\delta L/T_R$ of the central frequency of the signal field from the cavity resonance. The dynamics of the parametric process are described by the integral kernel $G(t, t')$, which is determined by the geometry and nonlinear properties of the crystal, dispersion, as well as temporal and spatial properties of the pump field [28]. The parameter $D = \sqrt{\mathcal{R}}k''(\omega_0)L/(2T_R)$ sets the magnitude of group velocity dispersion in the resonant cavity medium. Furthermore, vacuum field entering the resonant cavity input mirror is described by the operator $\hat{A}^{\text{in}}(t, T)$. This defines the Langevin noise, whose only non-zero correlation function is given by:

$$\langle \hat{A}^{\text{in}}(t, T) \hat{A}^{\text{in}\dagger}(t', T') \rangle = T_R \delta(t - t') \delta(T - T').$$

The output field of the system is related to the fields inside and outside the resonant cavity through the standard input-output relation:

$$\hat{A}^{\text{out}}(t, T) + \hat{A}^{\text{in}}(t, T) = \sqrt{\gamma T_R} \hat{A}(t, T).$$

It has been shown [18,29] that under certain experimental conditions, the eigenfunctions of the kernel $G(t, t')$ are described by Hermite-Gauss polynomials:

$$s_n(t) = \frac{i^n}{\sqrt{\tau_s 2^n n! \sqrt{\pi}}} H_n(t/\tau_s) e^{-t^2/2\tau_s^2},$$

where τ_s is the full width at half maximum (FWHM) of the Gaussian (fundamental) mode in the time domain. The set of functions $\{s_n(t)\}$ is complete, allowing it to be used as a basis for expanding the signal field inside the resonant cavity [30–32]:

$$\hat{A}(t, T) = \sum_{n \geq 0} \hat{a}_n(T) s_n(t),$$

where the expansion coefficients $\{\hat{a}_n(T)\}$ are bosonic creation and annihilation operators of photons in the parametric modes: $[\hat{a}_n(T), \hat{a}_m^\dagger(T')] = T_R \delta_{n,m} \delta(T - T')$.

The expansion (2) allows transitioning to a system of differential equations describing the evolution of the amplitudes $\hat{a}_n(T)$ of the parametric modes of the radiation:

$$\frac{\partial \hat{a}_n(T)}{\partial T} = \left(-\frac{\gamma}{2} + i(\Delta - C_{n,n}) \right) \hat{a}_n(T) + \frac{\lambda_n}{2} \hat{a}_n^\dagger(T) - i \sum_{m \neq n} C_{n,m} \hat{a}_m(T) + \sqrt{\frac{\gamma}{T_R}} \hat{a}_n^{\text{in}}(T), \quad (3)$$

where λ_n is the real eigenvalue of the parametric kernel corresponding to the eigenfunction $s_n(t)$. According to (1), the coefficients $C_{n,m}$ are determined as overlap integrals of parametric modes of the following form:

$$C_{n,m} = D \int_{-\infty}^{+\infty} s_n^*(t) \frac{\partial^2}{\partial t^2} s_m(t) dt. \quad (4)$$

Properties of Hermite-Gauss polynomials imply that in the system (3), only mode amplitudes with the same parity of their indices are coupled, with the coupling strength defined by real coefficients:

$$O_{n,m} \tau_s^2 = -\frac{2n-1}{2} \delta_{n,m} - \frac{\sqrt{(n-1)n}}{2} \delta_{n-2,m} - \frac{\sqrt{(n+1)(n+2)}}{2} \delta_{n+2,m},$$

where $O_{n,m}$ is the overlap integral of the modes in (4).

Thus, the radiation in the SPOPO resonant cavity can be considered as an ensemble of coupled parametric modes, each characterized by the following set of quantities: the amplitude operator $\hat{a}_n(T)$, parametric pumping λ_n , detuning from resonance $\Delta_n = \Delta - C_{n,n}$, loss coefficient γ , as well as the Langevin noise operator $\hat{f}_n(T) = \sqrt{\frac{\gamma}{T_R}} \hat{a}_n^{\text{in}}(T)$. The amplitudes of the parametric radiation modes at the system output are given by the relation [28]:

$$\hat{a}_n^{\text{out}}(T) + \hat{a}_n^{\text{in}}(T) = \sqrt{\gamma T_R} \hat{a}_n(T).$$

Average photon number in parametric modes

In [28] it was shown that the solution of system (3) can be obtained in the frequency domain using an approach analogous to perturbation theory. Assuming that the mode coupling induced by group velocity dispersion is sufficiently small, one can obtain a solution of order K in terms of coupling coefficients in the following form:

$$\hat{a}_n^{\text{out}}(\Omega) = W_n(\Omega) \hat{f}_n(\Omega) + V_n(\Omega) \hat{f}_n^\dagger(\Omega) + \sum_{k=1}^K \hat{h}_n^{(k)}(\Omega),$$

where

$$\hat{h}_n^{(k)}(\Omega) = \sum_{m_1} \cdots \sum_{m_k} \left[U_{m_1, \dots, m_k}(\Omega) \hat{f}_{m_k}(\Omega) V_{m_1, \dots, m_k}(\Omega) \hat{f}_{m_k}^\dagger(-\Omega) \right].$$

Here, the coefficients $W_n(\Omega)$, $U_{m_1, \dots, m_k}(\Omega)$ and $V_{m_1, \dots, m_k}(\Omega)$ depend on the chosen pump configuration in the parametric modes, the resonator geometry, and the nonlinear crystal.

A key property of these functions is their proportionality to the mode coupling coefficients $C_{n,m}$ established by the following rule:

$$U_n(\Omega), W_n(\Omega), V_n(\Omega) \propto C_{nn}^0;$$

$$U_{m_1, m_2, \dots, m_k}(\Omega), V_{m_1, m_2, \dots, m_k}(\Omega) \propto C_{m_1, m_2} C_{m_2, m_3} \cdots C_{m_{k-1}, m_k},$$

Their explicit form is given in [28].

In the present work, we will calculate the average photon numbers in parametric modes and investigate their dependence on the magnitude of group velocity dispersion:

$$n_n(T) = \langle \hat{a}_n^{\text{out} \dagger}(T) \hat{a}_n^{\text{out}}(T) \rangle = \frac{1}{2\pi} \iint d\Omega d\Omega' e^{-i(\Omega - \Omega')T} \langle \hat{a}_n^{\text{out} \dagger}(\Omega) \hat{a}_n^{\text{out}}(\Omega') \rangle.$$

Using solution (5) and accounting for the correlation properties of the Langevin terms, one can write the desired correlator $\langle \hat{a}_n^{\text{out} \dagger}(\Omega) \hat{a}_n^{\text{out}}(\Omega') \rangle$ for the output field in the following compact form:

$$\langle \hat{a}_n^{\text{out} \dagger}(\Omega) \hat{a}_n^{\text{out}}(\Omega') \rangle = \frac{\gamma T_R}{2\pi} S(\Omega) \delta(\Omega - \Omega').$$

Then the average photon number in a mode is given by the integral

$$n_n(T) = \frac{\gamma T_R}{2\pi} \int d\Omega S(\Omega) = n_n.$$

This quantity does not depend on time. Thus, by calculating the function $S(\Omega)$, one can find the average photon number in the mode with index n at an arbitrary order of perturbation theory. The zeroth-order contribution in the coupling coefficients has the form:

$$S^{(0)}(\Omega) = \gamma |V_n(\Omega)|^2.$$

The second-order smallness terms are:

$$S^{(2)}(\Omega) = \gamma \sum_{m \neq n} \left\{ V_n^*(\Omega) V_{n,m,n}(\Omega) + V_{n,m}^*(\Omega) V_{n,m}(\Omega) + V_n(\Omega) V_{n,m,n}^*(\Omega) \right\}.$$

The fourth-order smallness terms are:

$$S^{(4)}(\Omega) = \gamma \sum_{m \neq n} \sum_{m' \neq n} \sum_{p \neq m, m'} \left\{ V_n^*(\Omega) V_{n,m',p,m,n}(\Omega) + V_{n,m}^*(\Omega) V_{n,m',p,m}(\Omega) + V_{n,m,p}^*(\Omega) V_{n,m',p}(\Omega) + V_{n,m}(\Omega) V_{n,m',p,m}^*(\Omega) + V_n(\Omega) V_{n,m',p,m,n}^*(\Omega) \right\},$$

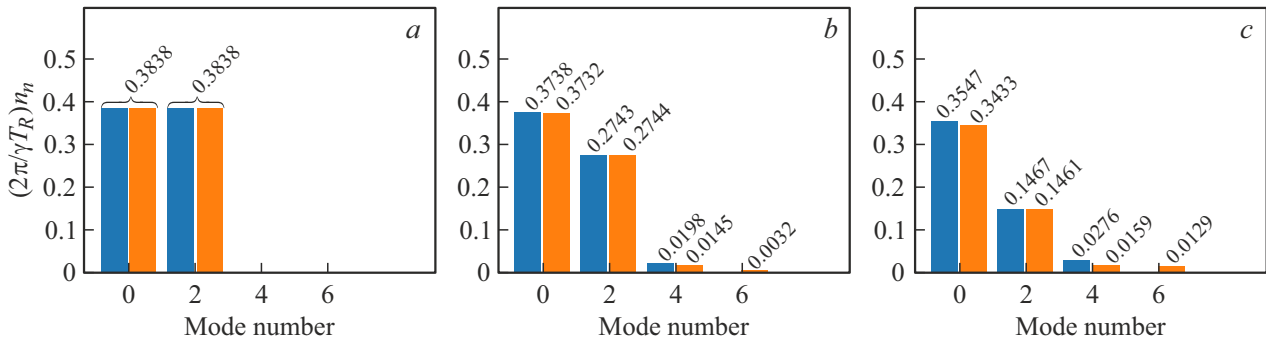


Figure 2. Distribution of the average photon number in the first four even parametric radiation modes for various values of group velocity dispersion, calculated at the second (blue) and fourth (orange) orders of perturbation theory in coupling coefficients. Parametric amplification occurs equally in modes 0 and 2: $\lambda_0/\gamma = \lambda_2/\gamma = 0.33$. The considered dispersion values are *a* — $C_{n,m}/\gamma = 0$, *b* — $C_{b,n}/\gamma = 0.10 O_{n,m} \tau_s^2$, *c* — $C_{n,m}/\gamma = 0.25 O_{n,m} \tau_s^2$.

and so on. All odd-order contributions in $C_{n,m}$ to the quantity $n_n(T)$ are identically zero. In this work, we restrict ourselves to terms up to the fourth order in smallness and will numerically demonstrate that this consideration provides a satisfactory result for most admissible dispersion values.

Numerical modeling

We will use SPOPO parameters matched to the experimental work [19]. For example, we assume the full width at half maximum (FWHM) of the fundamental mode is 8.5 nm, corresponding to a duration $\tau_s = 67$ fs. The attenuation coefficients in the modes are $\gamma/2\pi = 3$ MHz, and the pump pulse repetition rate is $T_R^{-1} = 76$ MHz. The value of group velocity dispersion will be set by varying the parameter D in (4). The dispersion value corresponding to experimental parameters is given as $C_{n,m}/\gamma = 0.25 O_{n,m} \tau_s^2$. Additionally, we assume that the pump pulses and nonlinear medium properties are selected such that parametric excitation occurs only in a particular set of modes among the considered N first modes.

Figure 2 shows the photon distribution in parametric modes in a system supporting the first seven Hermite-Gauss modes. In subsequent modeling results, we will assume resonance detuning in the system is absent, i.e., $\Delta = 0$, unless stated otherwise. Pumping is arranged such that parametric amplification occurs only in modes numbered 0 and 2. The pump magnitude is set as $\lambda_0/\gamma = \lambda_2/\gamma = 0.33$, corresponding to 6 dB squeezing in the absence of dispersion in the crystal material. It can be seen that when dispersion is absent (Fig. 2, *a*), the average photon numbers are equal in modes 0 and 2, while other modes supported by the resonant cavity remain in the vacuum state. The picture changes when group velocity dispersion is present, which leads to detuning of parametric modes from resonance and to their linear coupling. Specifically, the average photon number in the second mode decreases compared to the fundamental mode

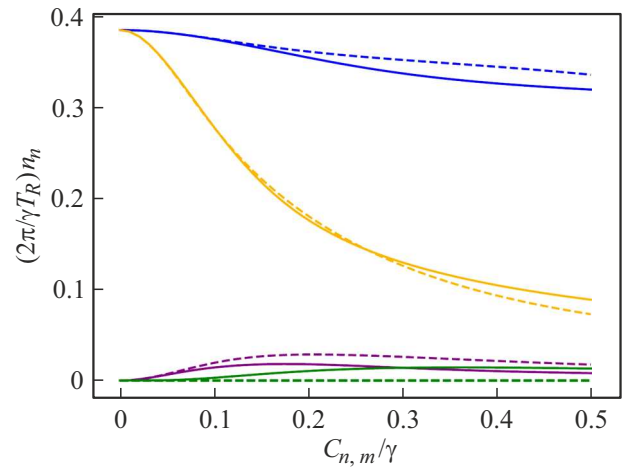


Figure 3. Distributions of the average photon number in the first four even parametric radiation modes for various group velocity dispersion values, calculated at second (dashed lines) and fourth (solid lines) orders of perturbation theory in coupling coefficients. Pumping of the modes is uniform and equal to $\lambda_0/\gamma = \lambda_2/\gamma = 0.33$. Colors indicate different radiation modes: zero (blue), second (yellow), fourth (violet), sixth (green).

(Fig. 2, *b*). This effect is due to dispersion-induced coupling of the second mode with mode number 4, described by the coefficient C_{24} . Since $C_{02} < C_{24}$, the second parametric mode transfers more photons to the fourth mode (which is not pumped) than it receives from the fundamental mode, causing the average photon number in the fundamental mode to exceed that of the others. Furthermore, taking into account the fourth-order terms in coupling coefficients leads to additional photon transfer from the fourth to the sixth parametric mode (Fig. 2, *b, c*). Due to an even larger value of this coupling, the percentage ratio of photon exchange among these modes becomes even more significant. This effect intensifies with increasing dispersion magnitude, as clearly seen by comparing Fig. 2, *b* and *c*.

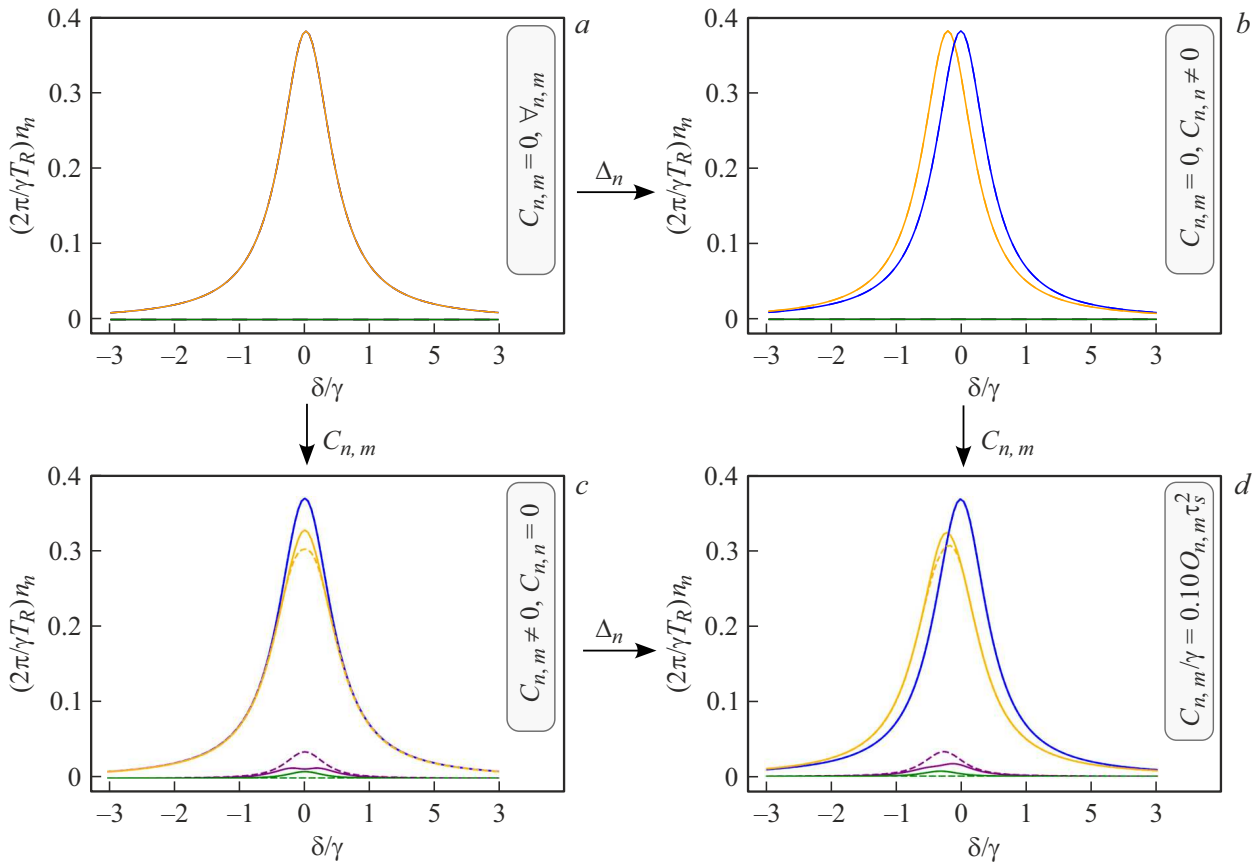


Figure 4. Distributions of average photon number in the first four even radiation modes considering various dispersion effects: no dispersion (*a*), accounting for dispersion-induced detuning of modes (*b*), accounting for dispersion-induced mode coupling (*c*), and accounting for both effects (*d*). Calculations were performed at second (dashed lines) and fourth (solid lines) orders of perturbation theory in coupling coefficients. Pumping of the modes is uniform and equal to $\lambda_0/\gamma = \lambda_2/\gamma = 0.33$. Colors indicate different radiation modes: zero (blue), second (yellow), fourth (violet), sixth (green).

A more complete picture showing the distribution of average photon number among radiation modes as a function of dispersion magnitude is presented in Fig. 3. The pumping regime is the same as in Fig. 2. It is worth noting that changes in parametric amplification magnitude, either increasing or decreasing, do not alter the shape of the dependence in Fig. 3; such manipulations lead only to a corresponding vertical scaling. It is also observed that as dispersion increases, the number of photons in parametric modes decreases monotonically. This effect is explained by increased detuning of modes from resonance with dispersion growth and, consequently, less efficient parametric excitation of modes. Additionally, at some dispersion value, the photon number in the sixth radiation mode exceeds that in the fourth mode, i.e., the magnitude of dispersion-induced coupling increases so much that the fourth mode transfers photons faster than it receives them from the adjacent pumped mode.

Figure 4 shows the photon number in parametric modes as a function of resonant cavity detuning Δ . At zero dispersion, the spectrum of average photon number in the pumped radiation modes forms a Lorentzian contour, shown

in Fig. 4, *a*. Group velocity dispersion leads to two related processes: detuning of parametric modes from resonance and the emergence of dispersion-induced coupling between them. The influence of these two processes on photon numbers in parametric modes is analyzed separately in Fig. 4, *b* and *c*. Specifically, Fig. 4, *b* shows that in the absence of mode coupling, the overall spectral structure remains unchanged. However, due to additional dispersion-induced detuning in each mode, expressed by the quantity $C_{n,n}$ resonance for the various pumped modes occurs at different detuning values Δ . On the other hand, considering only the coupling between parametric modes results in a much more complex spectral pattern (Fig. 4, *c*), which remains symmetric about the $\Delta = 0$ value. A significant discrepancy between the second- and fourth-order solutions in coupling coefficients is observed, likely caused by fundamental limitations of the applied theoretical approach, indicating restrictions of the perturbation theory used. Fig. 4, *d* shows the photon number distribution when both processes due to the presence of dispersion are accounted for simultaneously. A shift and distortion of the Lorentzian contour are observed for each parametric

mode. Moreover, the solutions of second and fourth order in this case differ significantly and even reach negative values, which indicates the necessity of further studies in this area to enable effective control over the characteristics of the generated radiation.

Conclusion

The influence of group velocity dispersion in the resonant cavity of a synchronously pumped optical parametric generator on the distribution of the average photon number across the radiation modes has been studied. The theoretical part of this research was based on two main methods. First, we used an approach allowing to represent the field as a set of eigenmodes of the spontaneous parametric scattering process [30–32], between which a linear coupling is observed in the presence of dispersion. Second, as a method for solving the previously constructed field evolution equations, we applied a technique analogous to the development of perturbation theory in the coupling coefficients of the equations describing the evolution of quantum parametric oscillators [28]. As a result, an expression was obtained describing the average photon number in each parametric mode up to an arbitrary predetermined order in the smallness of the mode coupling coefficients. Based on this expression, an analysis of the photon number distribution across the radiation modes and its dependence on various task parameters was conducted. In particular, it was established that with increasing dispersion, the total number of photons in the parametric modes decreases, which is caused by the detuning of the modes from resonance and the reduction in efficiency of the parametric process. Furthermore, accounting for dispersion leads to a redistribution of photons among the investigated radiation modes due to the aforementioned coupling of parametric modes. The overall pattern of this redistribution does not depend on the magnitude of gain present in the system. It should also be noted that dispersion significantly affects the photon number distributions over the modes in the presence of detuning from resonance.

Funding

This study was carried out with the support of the Russian Science Foundation (grant №. 24-22-00318).

Conflict of interest

The authors declare that they have no conflict of interest.

References

- [1] A.I. Lvovsky. *Squeezed light* (2014). DOI: 10.48550/ARXIV.1401.4118
- [2] O. Crisafulli, N. Tezak, D.B.S. Soh, M.A. Armen, H. Mabuchi. *Optics Express*, **21**, 18371 (2013). DOI: 10.1364/OE.21.018371
- [3] F. Kaiser, B. Fedrici, A. Zavatta, V.D. Auria, S. Tanzilli. *Optica*, **3**, 362 (2016). DOI: 10.1364/OPTICA.3.000362
- [4] W. Asavanant et al. *Science*, **366**, 373 (2019). DOI: 10.1126/science.aay2645
- [5] I. Walmsley. *Optica Quantum*, **1**, 35 (2023). DOI: 10.1364/OPTICAQ.507527
- [6] A.E. Ulanov et al. *Nature Communications*, **7**, 11925 (2016). DOI: 10.1038/ncomms11925
- [7] A. Avella et al. *Optics Express*, **19**, 23249 (2011). DOI: 10.1364/OE.19.023249
- [8] M. Manceau et al. *Physical Review Letters*, **119**, 223604 (2017). DOI: 10.1103/PhysRevLett.119.223604
- [9] W. Yang et al. *Chemosensors*, **11**, 18 (2022). DOI: 10.3390/chemosensors11010018
- [10] R. Gosalia, R. Malaney, R. Aguinaldo, J. Green, P. Brereton. In *GLOBECOM 2023 — 2023 IEEE Global Communications Conference* (IEEE, Kuala Lumpur, Malaysia, 2023) p. 2317–2322. DOI: 10.1109/GLOBECOM54140.2023.10437698
- [11] J. Aasi et al. *Nature Photonics*, **7**, 613 (2013). DOI: 10.1038/nphoton.2013.177
- [12] L.-A. Wu, H.J. Kimble, J.L. Hall, H. Wu. *Physical Review Letters*, **57**, 2520 (1986). DOI: 10.1103/PhysRevLett.57.2520
- [13] C. Fabre N. Treps. *Reviews of Modern Physics*, **92**, 035005 (2020). DOI: 10.1103/RevModPhys.92.035005
- [14] M. Piccardo et al. *Journal of Optics*, **24**, 013001 (2022). DOI: 10.1088/2040-8986/ac3a9d
- [15] V. Sukharnikov, P. Sharapova, O. Tikhonova. *Optics & Laser Technology*, **136**, 106769 (2021). DOI: 10.1016/j.optlastec.2020.106769
- [16] T. Kouadou, F. Sansavini, M. Ansquer, J. Henaff, N. Treps, V. Parigi. *APL Photonics*, **8**, 086113 (2023). DOI: 10.1063/5.0156331
- [17] A.D. Manukhova, K.S. Tikhonov, T.Y. Golubeva, Y.M. Golubev. *Physical Review A*, **96**, 023851 (2017). DOI: 10.1103/PhysRevA.96.023851
- [18] G. Patera, N. Treps, C. Fabre, G.J. De Valcárcel. *The European Physical Journal D*, **56**, 123 (2010). DOI: 10.1140/epjd/e2009-00299-9
- [19] J. Roslund et al. *Nature Photonics*, **8**, 109 (2014). DOI: 10.1038/nphoton.2013.340
- [20] B. Lamine, C. Fabre, N. Treps. *Physical Review Letters*, **101**, 123601 (2008). DOI: 10.1103/PhysRevLett.101.123601
- [21] S. Wang, X. Xiang, N. Treps, C. Fabre, T. Liu, S. Zhang, R. Dong. *Physical Review A*, **98**, 053821 (2018). DOI: 10.1103/PhysRevA.98.053821
- [22] Y. Cai, J. Roslund, V. Thiel, C. Fabre, N. Treps. *npj Quantum Information*, **7**, 82 (2021). DOI: 10.1038/s41534-021-00419-w
- [23] N.C. Menicucci. *Physical Review Letters*, **112**, 120504 (2014). DOI: 10.1103/PhysRevLett.112.120504
- [24] V.A. Averchenko, T.Y. Golubeva, Y.M. Golubev, C. Fabre. *Optics and Spectroscopy*, **105**, 758 (2008). DOI: 10.1134/S0030400X08110192
- [25] M. Walschaers, B. Sundar, N. Treps, L.D. Carr, V. Parigi. *Quantum Science and Technology*, **8**, 035009 (2023). DOI: 10.1088/2058-9565/accdfd

- [26] P. Renault, J. Nokkala, G. Roeland, N. Joly, R. Zambrini, S. Maniscalco, J. Piilo, N. Treps, V. Parigi. *PRX Quantum*, **4**, 040310 (2023). DOI: 10.1103/PRXQuantum.4.040310
- [27] V. Roman-Rodriguez, D. Fainsin, G.L. Zanin, N. Treps, E. Diamanti, V. Parigi. *Multimode Squeezed State for Reconfigurable Quantum Networks at Telecommunication Wavelengths* (2023). DOI: 10.48550/ARXIV.2306.07267
- [28] V.A. Averchenko, D.M. Malyshev, K.S. Tikhonov. *New Journal of Physics*, **26**, 123017 (2024). DOI: 10.1088/1367-2630/ad9be1
- [29] F. Arzani, C. Fabre, N. Treps. *Physical Review A*, **97**, 033808 (2018). DOI: 10.1103/PhysRevA.97.033808
- [30] K.J. Blow, R. Loudon, S.J.D. Phoenix, T.J. Shepherd. *Physical Review A*, **42**, 4102 (1990). DOI: 10.1103/PhysRevA.42.4102
- [31] B. Brecht, D.V. Reddy, C. Silberhorn, M. Raymer. *Physical Review X*, **5**, 041017 (2015). DOI: 10.1103/PhysRevX.5.041017
- [32] D.B. Horoshko, L. La Volpe, F. Arzani, N. Treps, C. Fabre, M.I. Kolobov. *Physical Review A*, **100**, 013837 (2019). DOI: 10.1103/PhysRevA.100.013837

Translated by J.Savelyeva